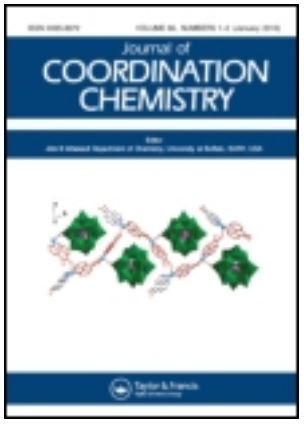

Journal of Coordination Chemistry
Publication details, including instructions for authors and subscription information:
http://www.tandfonline.com/loi/gcoo20

Preparation and characterization of four polymeric metal complexes based on the flexible ligand 1H-1,2,4-triazole-1-propionic acid in different conformations

Zhong Zhang [a], Di-Feng Wu [a], Kun Hu [a], Yun-Jia Shi [a], Zi-Lu Chen [a] & Fu-Pei Liang [a]

[a] Key Laboratory for the Chemistry and Molecular Engineering of Medicinal Resources (Ministry of Education of China), School of Chemistry and Chemical Engineering of Guangxi Normal University, Guilin, P.R. China

Accepted author version posted online: 22 May 2013.Published online: 25 Jun 2013.

To cite this article: Zhong Zhang, Di-Feng Wu, Kun Hu, Yun-Jia Shi, Zi-Lu Chen & Fu-Pei Liang (2013) Preparation and characterization of four polymeric metal complexes based on the flexible ligand 1H-1,2,4-triazole-1-propionic acid in different conformations, Journal of Coordination Chemistry, 66:14, 2499-2515, DOI: 10.1080/00958972.2013.807919

To link to this article: http://dx.doi.org/10.1080/00958972.2013.807919

Journal of Coordination Chemistry, 2013
Vol. 66, No. 14, 2499–2515, http://dx.doi.org/10.1080/00958972.2013.807919

Preparation and characterization of four polymeric metal complexes based on the flexible ligand 1*H*-1,2,4-triazole-1-propionic acid in different conformations

ZHONG ZHANG*, DI-FENG WU, KUN HU, YUN-JIA SHI, ZI-LU CHEN and FU-PEI LIANG

Key Laboratory for the Chemistry and Molecular Engineering of Medicinal Resources (Ministry of Education of China), School of Chemistry and Chemical Engineering of Guangxi Normal University, Guilin, P.R. China

(*Received 28 July 2012; in final form 28 March 2013*)

Three 2-D layered coordination polymers with (4,4) topology, $\{[Cu(trzp)_2(H_2O)]\cdot 1.18H_2O\}_n$ (**1**), $\{[Co(trzp)_2(H_2O)_2]\cdot 2H_2O\}_n$ (**2**), and $\{[Cd(trzp)_2(H_2O)]\cdot 2H_2O\}_n$ (**3**), have been synthesized with the flexible, bifunctional ligand 1*H*-1,2,4-triazole-1-propionate ($trzp^-$) as a two-connected bridge. In addition, a complicated 3-D MOF $[Ag_3(trzp)_2(NO_3)]_n$ (**4**) has been obtained with the help of Ag···Ag interactions and $trzp^-$ as a four-connected linker. Htrzp and **1**–**4** have been characterized by single-crystal X-ray diffraction, elemental analysis, and infrared spectroscopy. The structural analysis showed that Htrzp has a *gauche* conformation in the solid state. However, both *gauche* and *trans* conformers of $trzp^-$ are observed in the crystals of **1**; only one conformer of $trzp^-$ exists in the other three compounds (*trans* conformation in **2** and **3**, and *gauche* conformation in **4**). The thermal behaviors of **1**–**4** have been examined by thermal gravimetric analysis under nitrogen, which revealed that metal cyanide salts $M(CN)_n$ (M = Cu(II), Co(II), Cd(II), and Ag(I), $n = 1$ or 2) may be an intermediate pyrolytic decomposition product of the corresponding compounds.

Keywords: Preparation; Crystal structure; 1*H*-1,2,4-Triazole-1-propionic acid; Conformational flexibility

1. Introduction

The preparation of metal-organic frameworks (MOFs) with fascinating architectures and promising applications as functional materials has been a hot research topic in coordination chemistry as well as materials science over the past decade [1, 2]. From the numerous investigations on the preparation of MOFs, it can be concluded that many factors, such as the coordination number and geometry of the metal center, ligating ability of the counterion, presence of the templating agents, and selected reaction conditions, influence the structures and properties of MOFs [3–7]. Among these factors, the structural characteristics of the organic connectors have been proven to play a pivotal role [8]. Thus, the

*Corresponding author. Email: zhangzhong@mailbox.gxnu.edu.cn

careful selection of the appropriate organic linkers with distinct shapes and coordination preferences is critical for the construction of MOFs with desired structures and properties.

Triazole heterocycles and carboxylic acid ligands have individually been shown to have potential in the fabrication of MOFs due to the excellent coordination capabilities and distinct coordination modes [9–15]. Accordingly, the combination of triazole heterocycles and carboxylic acid moieties may provide a new family of mixed N, O-donor organic ligands exhibiting more abundant coordination modes, as well as binding affinity toward both transition and rare earth metals. Recently, efforts contributing to the self-assembly of these multifunctional building blocks with different metal salts have been reported [16–24]. As an expansion of these studies, we have used the bifunctional building block, 1*H*-1,2,4-triazole-1-propionic acid (Htrzp), which has a flexible propionic acid group. Besides the various coordination patterns, Htrzp may assume different conformations from rotation about the central C–C bond in the ethylene spacer. Therefore, the structural flexibility and conformational changes of the ligand may be considered as available structural factors controlling the framework topologies of the resulting coordination polymers. Through the reaction between Htrzp and a series of transition metal salts, three 2-D coordination polymers, $\{[Cu(trzp)_2(H_2O)]\cdot 1.5H_2O\}_n$ (**1**), $\{[Co(trzp)_2(H_2O)_2]\cdot 2H_2O\}_n$ (**2**), and $\{[Cd(trzp)_2(H_2O)]\cdot 2H_2O\}_n$ (**3**), and a 3-D MOF, $[Ag_3(trzp)_2(NO_3)]_n$ (**4**), have been isolated. The solid-state structures of these compounds have been determined *via* single-crystal X-ray diffraction, and the versatile coordination geometries (scheme 1) and different steric conformations (scheme 2) of $trzp^-$ are discussed on the basis of the structural characterization. The thermal stabilities of all compounds have been investigated under a nitrogen atmosphere. Furthermore, structural comparisons between these complexes and related compounds constructed with a ligand with a shorter spacer, 1*H*-1,2,4-triazole-1-acetic acid (Htrza), are provided.

2. Experimental

2.1. *Materials and measurements*

Htrzp was synthesized according to a published method [25]. All other chemicals employed in this study were of analytical grade and used as received. C, H, N elemental analyses were performed on a PE 2400 II analyzer. IR spectra were recorded as KBr disks

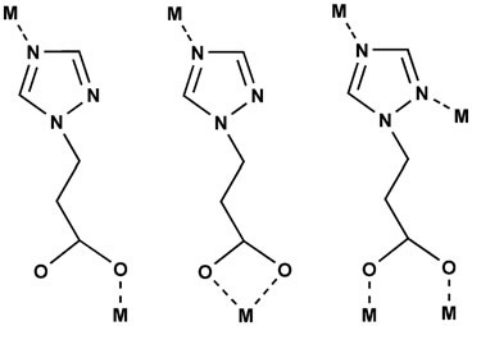

Scheme 1. A representation of the linkage patterns of $trzp^-$ in **1**–**4**. 47 × 25 mm (600 × 600 DPI).

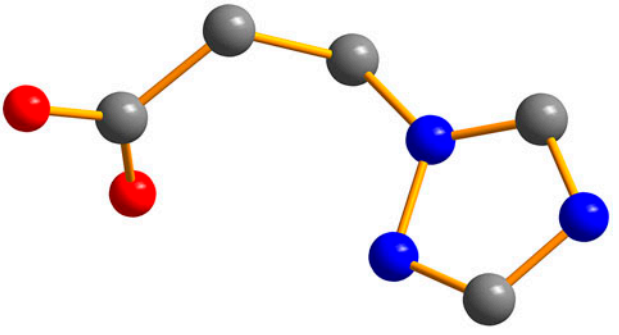

gauche conformation

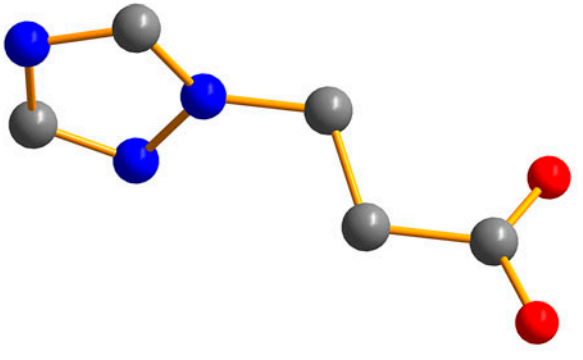

trans conformation

Scheme 2. Two different conformations of $trzp^-$ in **1**–**4**.

on a Nicolet 360 FT-IR spectrometer in the 400–4000 cm^{-1} spectral region. Powder X-ray diffraction (PXRD) experiments were carried out using a Rigaku D/Max-2500 V diffractometer with monochromated Cu K_a radiation at room temperature. Thermogravimetric analyses (TGA) were carried out on a PerkinElmer Pyris Diamond TG/DTA instrument at a heating rate of 10 °C min^{-1} under a nitrogen atmosphere.

2.2. *Synthesis*

2.2.1. Synthesis of $\{[Cu(trzp)_2(H_2O)]\cdot 1.18H_2O\}_n$ (1). A solution of $Cu(OAc)_2\cdot 2H_2O$ (45 mg, 0.2 mM) in water (6 mL) was added dropwise to an aqueous solution (5 mL) of Htrzp (56 mg, 0.4 mM). The resulting mixture was heated at 65 °C for 4 h with vigorous stirring. The solution was filtered, and the filtrate was left to evaporate at room temperature in air. After three weeks, deep blue, block-shaped crystals suitable for X-ray analysis formed in 62% yield. Anal. Calcd for $C_{10}H_{16.36}CuN_6O_{6.18}$ (%): C, 31.35; H, 4.30; N, 21.94. Found (%): C, 30.89; H, 4.34; N, 21.71. FT-IR (KBr, cm^{-1}): 3413(br), 3128(m), 1583(s), 1533(m), 1454(w), 1406(s), 1385(m), 1297(w), 1283(w), 1217(w), 1126(s), 1022(w), 1005(w), 672(m), 571(w).

2.2.2. Synthesis of $\{[Co(trzp)_2(H_2O)_2]\cdot 2H_2O\}_n$ (2). $Co(OAc)_2\cdot 4H_2O$ (75 mg, 0.3 mM) and Htrzp (85 mg, 0.6 mM) were mixed in water (18 mL) to give a purple solution, which was stirred at 65 °C for 4 h. After filtration, the filtrate was allowed to evaporate at room temperature in air. Red, block-shaped crystals were obtained in 73% yield after a month and a half. Anal. Calcd for $C_{10}H_{20}CoN_6O_8$ (%): C, 29.21; H, 4.90; N, 20.44. Found (%): C, 28.97; H, 4.52; N, 20.43. FT-IR (KBr, cm^{-1}): 3419(br), 3125(m), 1574(s), 1528(m), 1435(s), 1422(s), 1342(m), 1279(s), 1207(w), 1124(m), 1048(m), 996(m), 932(w), 836(w), 748(m), 674(m), 653(w), 500(w).

2.2.3. Synthesis of $\{[Cd(trzp)_2(H_2O)]\cdot 2H_2O\}_n$ (3). An aqueous solution (10 mL) of $Cd(NO_3)_2\cdot 2H_2O$ (54 mg, 0.2 mM) was slowly added to a stirred methanol solution (5 mL) of Htrzp (56 mg, 0.4 mM). Afterward, a dilute aqueous solution of NaOH (0.5 M L^{-1}) was added to adjust the mixture to pH 5, 6. The mixture was stirred at 65 °C for 4 h and then was cooled to room temperature and filtrated. A slow evaporation of the filtrate under ambient conditions gave colorless prismatic crystals suitable for X-ray analysis in 59% yield. Anal. Calcd for $C_{10}H_{18}CdN_6O_7$ (%): C, 26.89; H, 4.06; N, 18.81. Found (%): C, 26.75; H, 4.41; N, 18.93. FT-IR (KBr, cm^{-1}): 3446(br), 3143(m), 1590(s), 1525(m), 1443(w), 1393(s), 1360 (m), 1288(m), 1258(m), 1127(m), 1014(m), 995(m), 893(m), 806(w), 681(m), 671(m), 566(m).

2.2.4. Synthesis of $[Ag_3(trzp)_2(NO_3)]_n$ (4). An aqueous solution (10 mL) of Htrzp (56 mg, 0.4 mM) was mixed with an aqueous solution (8 mL) of $AgNO_3$ (102 mg, 0.6 mM) to give a colorless clear solution, which was stirred at 65 °C for 4 h. After cooling and filtration, the filtrate was allowed to stand in the dark to evaporate the solvent. Colorless block-like crystals were isolated from the solution in 33% yield after two weeks. Anal. Calcd for $C_{10}H_{12}Ag_3N_7O_7$ (%): C, 18.04; H, 1.82; N, 14.73. Found (%): C, 18.12; H, 1.68; N, 14.44. FT-IR (KBr, cm^{-1}): 3409(br), 3117(m), 1582(s), 1514(m), 1385(s), 1318(w), 1277(m), 1210(m), 1142(m), 1047(w), 1023(w), 965(w), 877(w), 680(m).

In general, the same metal complexes were obtained irrespective of the metal-to-ligand ratio (1 : 1, 1 : 1.5, 1 : 2) and the reaction temperature. Nevertheless, in most cases, the replacement of the preferred metal salts by different salts or a change of the solvent was unfavorable for the preparation of **1**–**4**. Complex **3** did not easily precipitate from an aqueous solution, and the addition of methanol was beneficial for its formation.

2.3. *X-ray crystallography*

The diffraction data for **1**–**4** were collected on a Bruker Smart APEX CCD area detector diffractometer with graphite-monochromated Mo K_α radiation ($\lambda = 0.71073$ Å) at 298 K. The structures were solved by direct methods and refined by full-matrix least-squares on F^2 using the *SHELXTL* program package [26]. All non-hydrogen atoms were refined anisotropically. The hydrogen atoms of the water molecules were located from difference Fourier maps and refined isotropically with the O–H bond length restrained to 0.85 Å; all other hydrogens were located in geometric positions and refined with a riding model. A disordered water molecule of crystallization in **1** was refined with an occupancy factor of

Table 1. Crystal data and structure refinement parameters for Htrzp and **1**–**4**.

Compound	Htrap	**1**	**2**	**3**	**4**
Empirical formula	$C_5H_7N_3O_2$	$C_{10}H_{16.36}CuN_6O_{6.18}$	$C_{10}H_{20}CoN_6O_8$	$C_{10}H_{18}CdN_6O_7$	$C_{10}H_{12}Ag_3N_7O_7$
Formula weight	141.14	383.07	411.25	446.70	665.88
Crystal system	Monoclinic	Monoclinic	Monoclinic	Orthorhombic	Monoclinic
Space group	$P2_1/c$	$P2_1/c$	$P2_1/c$	$Pbcn$	$C2/c$
Unit cell dimension (Å, °)					
a	5.5377(5)	9.3914(19)	8.1712(16)	13.760(3)	14.439(3)
b	13.779(3)	13.175(3)	13.958(3)	7.3499(15)	8.1937(16)
c	9.5312(14)	14.500(5)	7.4441(15)	15.494(3)	14.860(3)
α	90.00	90.00	90.00	90.00	90.00
β	114.83(1)	116.38(2)	111.08(3)	90.00	113.80(3)
γ	90.00	90.00	90.00	90.00	90.00
Volume (Å^3), Z	660.03(18), 4	1607.3(7), 4	792.2(3), 2	1566.9(5), 2	1608.6(6), 4
Absorption coeff. (mm^{-1})	0.113	1.400	1.140	1.443	3.672
Calculated density (g cm^{-3})	1.420	1.583	1.724	1.894	2.750
F (000)	296	787.2	426	896	1272
θ range for data collection (°)	2.96–26.50	3.09–25.00	3.04–27.48	3.02–27.48	3.00–27.47
Reflections collected	5085	13,438	8174	15,201	8279
Independent reflections	1353	2819	1814	1787	1847
	[R_{int} = 0.0238]	[R_{int} = 0.1499]	[R_{int} = 0.0825]	[R_{int} = 0.0363]	[R_{int} = 0.0435]
Data/restraints/parameters	1353/0/92	2819/1/218	1814/0/115	1787/0/111	1847/3/148
Goodness-of-fit on F^2	1.008	1.071	1.006	1.016	1.009
Final R indices [$I > 2\sigma(I)$]	R_1 = 0.0383	R_1 = 0.0818	R_1 = 0.0543	R_1 = 0.0258	R_1 = 0.0381
	wR_2 = 0.0824	wR_2 = 0.1575	wR_2 = 0.0884	wR_2 = 0.0709	wR_2 = 0.1086
R indices (all data)	R_1 = 0.0460	R_1 = 0.1348	R_1 = 0.0850	R_1 = 0.0311	R_1 = 0.0510
	wR_2 = 0.0862	wR_2 = 0.1758	wR_2 = 0.0975	wR_2 = 0.0741	wR_2 = 0.1167
Largest diff. peak/hole (eÅ^{-3})	0.216/−0.138	0.578/−0.630	0.353/−0.316	0.360/−0.301	0.720/−0.936

$R_1 = \Sigma||F_o| - |F_c||/|F_o|$. $wR_2 = \{\Sigma[w(F_o^2 - F_c^2)]^2/\Sigma[w(F_o^2)]^2\}^{1/2}$.

Table 2. Selected bond lengths (Å) and angles (°) for Htrzp and **1**–**4**.

Htrzp			
N1–N2	1.357(2)	C5–O2	1.199(2)
C5–O1	1.309(2)		
N2–C1–N3	114.6(1)	N2–C1–N3	110.4(1)
C2–N1–N2	109.7(1)	N2–N1–C3	121.0(1)
C1–N2–N1	102.4(1)	O2–C5–O1	123.6(1)
N1–C3–C4–C5	66.4(2)		
Complex **1**[a]			
Cu1–O1#1	1.965(5)	Cu1–O3#2	1.970(4)
Cu1–O5	2.514(6)	Cu1–N3	2.000(5)
Cu1–N6	2.003(5)		
O1#1–Cu1–N6	90.0(2)	O1#1–Cu1–N3	93.1(2)
O1#1–Cu1–O5	97.1(2)	O1#1–Cu1–O3#2	164.3(2)
O3#2–Cu1–O5	98.4(2)	O3#2–Cu1–N3	90.1(2)
O3#2–Cu1–N6	87.8(2)	N3–Cu1–O5	87.4(2)
N6–Cu1–O5	88.9(2)	N3–Cu1–N6	175.4(2)
N1–C3–C4–C5	175.9(6)	N4–C8–C9–C10	–88.5(8)
Complex **2**[b]			
Co1–O1	2.092(2)	Co1–O3	2.121(2)
Co1–N3	2.156(3)		
O1–Co1–O3	91.9(1)	O1–Co1–N3#2	90.9(1)
O1–Co1–O3#1	88.1(1)	O1–Co1–N3#3	89.1(1)
O3–Co1–N3#2	93.3(1)	O3–Co1–N3#3	86.7(1)
N1–C3–C4–C5	166.9(3)		
Complex **3**[c]			
Cd1–O1	2.501(2)	Cd1–O2	2.375(2)
Cd1–O3	2.366(3)	Cd1–N3#1	2.320(2)
O2–Cd1–O1	53.4(1)	O3–Cd1–O1	133.4(1)
O1–Cd1–N3#1	88.9(1)	O1–Cd1–N3#2	88.3(1)
O1–Cd1–O1#3	93.3(1)	O2–Cd1–O1#3	146.6(1)
O3–Cd1–O2	80.0(1)	O2–Cd1–N3#1	88.0(1)
O2–Cd1–N3#2	92.7(1)	O2#3–Cd1–O2	160.0(1)
O3–Cd1–N3#1	92.1(1)	N3#1–Cd1–N3#2	175.8(1)
N1–C3–C4–C5	–170.0(2)		
Complex **4**[d]			
Ag1–O3A	2.60(2)	Ag1–N2	2.424(5)
Ag1–O2#1	2.290(4)	Ag1–O1#2	2.286(4)
Ag2–N3	2.189(4)		
N2–Ag1–O3A	100.8(11)	O2#1–Ag1–N2	93.2(2)
O1#2–Ag1–N2	124.4(2)	O2#1–Ag1–O3A	88.0(4)
O1#2–Ag1–O3A	104.9(6)	O1#2–Ag1–O2#1	135.6(2)
N1–C3–C4–C5	–68.7(6)		

[a]Symmetry transformations used to generate equivalent atoms in **1**: #1 $x, 3/2-y, 1/2+z$; #2 $x, ½-y, -1/2+z$.
[b]Symmetry transformations used to generate equivalent atoms in **2**: #1 $-1-x, 1-y, -z$; #2 $-x, 1/2+y, ½-z$; #3 $-1+x, ½-y, -1/2+z$.
[c]Symmetry transformations used to generate equivalent atoms in **3**: #1 $½-x, ½-y, -1/2+z$; #2 $1/2+x, ½-y, -z$; #3 $1-x, y, -1/2-z$.
[d]Symmetry transformations used to generate equivalent atoms in **4**: #1 $x, 2-y, 1/2+z$; #2 $½-x, 1/2+y, ½-z$; #3 $½-x, -1/2+y, ½-z$.

0.18. Positional disorder of the oxygen atoms of the nitrate anion was observed in **4**. The crystal data and structure refinement parameters of **1**–**4** are listed in table 1. Selected bond lengths and angles for **1**–**4** are summarized in table 2. Selected hydrogen bond distances and angles in **1**–**3** are given in table 3.

Table 3. Selected hydrogen bond parameters for Htrzp and **1**–**3**.

D–H···A	*d*(D–H)	*d*(H···A)	*d*(D···A)	DHA
Htrzp[a]				
O(1)–H(1C)···N(3)#1	0.82	1.82	2.640(2)	172
Complex **1**[b]				
O(5)–H(5C)···O(2)#1	0.85	1.96	2.616(8)	133
O(5)–H(5D)···N(2)#2	0.85	2.07	2.880(8)	160
Complex **2**[c]				
O(3)–H(3C)···O(2)	0.85	1.98	2.723(4)	145
O(3)–H(3D)···N(2)#1	0.85	2.06	2.896(4)	167
O(4)–H(4C)···O(1)#2	0.85	2.23	2.956(4)	143
O(4)–H(4C)···O(3)#1	0.85	2.60	3.141(4)	123
O(4)–H(4D)···O(2)#3	0.85	2.06	2.898(4)	167
Complex **3**[d]				
O(3)–H(3C)···N(2)#1	0.85	2.02	2.834(2)	160
O(4)–H(4C)···O(2)#2	0.85	2.09	2.886(3)	155
O(4)–H(4D)···O(1)#3	0.85	2.08	2.921(3)	171

[a]Symmetry transformations used to generate equivalent atoms in Htrzp: #1 $-x$, $1/2+y$, $\frac{1}{2}-z$.
[b]Symmetry transformations used to generate equivalent atoms in **1**: #1 x, $-1/2-y$, $1/2+z$; #2 $-x$, $-y$, $-z$.
[c]Symmetry transformations used to generate equivalent atoms in **2**: #1 $-x$, $1-y$, $1-z$; #2 $1+x$, y, $1+z$; #3 $1+x$, y, z; #4 x, $\frac{1}{2}-y$, $1/2+z$.
[d]Symmetry transformations used to generate equivalent atoms in **3**: #1 x, $-y$, $-1/2+z$; #2 $1-x$, $1+y$, $\frac{1}{2}-z$; #3 $1-x$, y, $\frac{1}{2}-z$; #4 $\frac{1}{2}-x$, $1/2+y$, z.

3. Results and discussion

3.1. *Description of the crystal structures*

3.1.1. Crystal structure of Htrzp. The molecular structure of the flexible bifunctional ligand Htrzp is depicted in figure 1. The five-membered triazole ring is planar with a mean deviation of 0.0007 Å, and the carboxylic group lies almost perpendicular to the azole ring with a dihedral angle of 89.33°. The compound prefers a *gauche* conformation about the central C3–C4 bond with a torsion angle of N1–C3–C4–C5 = 66.4(2)°. The carboxylic OH group of one molecule forms an intermolecular hydrogen bond with N3 of a triazole ring in a neighboring molecule. Through the hydrogen bond interaction, Htrzp molecules are linked into a 1-D wave-like chain extending along the *b* axis. The π–π stacking interactions (centroid–centroid distance = 3.617 Å) between adjacent 1-D chains generate a 2-D supramolecular network (figure 2).

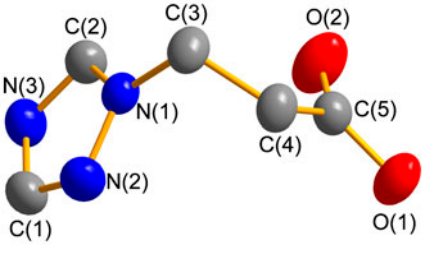

Figure 1. The molecular structure of Htrzp with thermal ellipsoids drawn at 50% probability. All hydrogens are omitted for clarity.

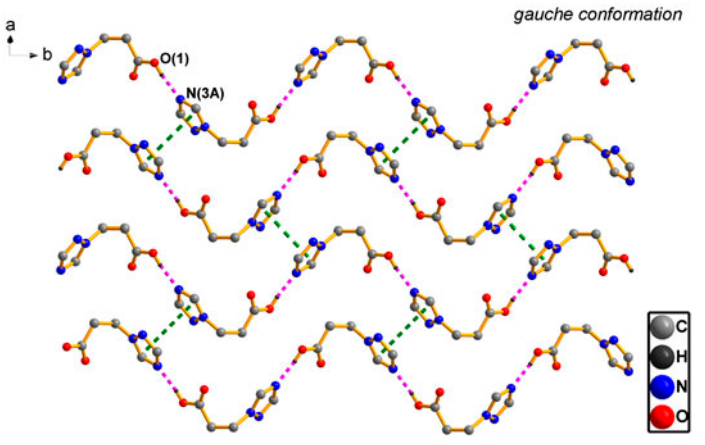

Figure 2. The 2-D layer of Htrzp linked by π–π stacking interactions and hydrogen bonds (dashed lines). (Symmetry codes: A: $-x$, $1/2+y$, $\frac{1}{2}-z$).

3.1.2. Crystal structure of $\{[Cu(trzp)_2(H_2O)]\cdot 1.18H_2O\}_n$ (1). X-ray structure analysis revealed that **1** crystallizes in the monoclinic space group $P2_1/c$ and forms a 2-D layer network. A Cu(II) center, two independent $trzp^-$ ligands, one coordinated water molecule, and a fully and a partially occupied lattice water molecule are present in the asymmetric unit (figure 3). The central Cu(II) ion resides in a square pyramidal coordination sphere, surrounded by two triazole N atoms (N3 and N6) from two $trzp^-$ ligands, two carboxylate O donors (O1A and O3B) from another two ligands, and one O atom (O5) of the coordinated water molecule. The equatorial plane of the pyramid is composed of N3, N6, O1A, and O3B with bond lengths ranging from 1.965(5) to 2.003(5) Å. All the bond distances

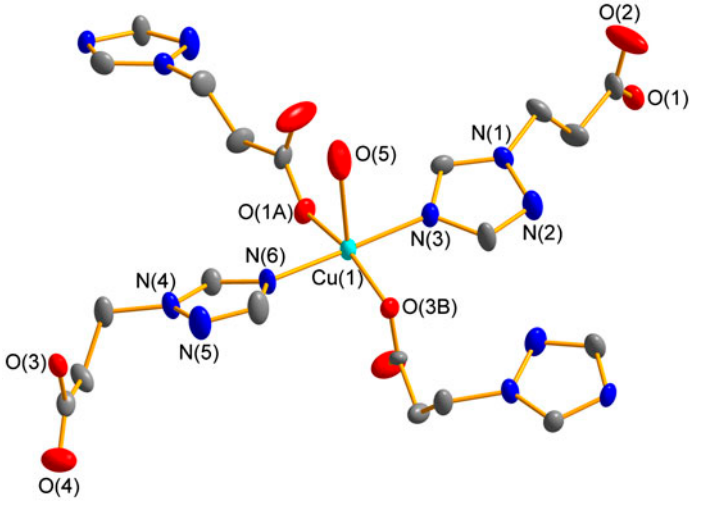

Figure 3. Coordination environment of Cu(II) in **1** with thermal ellipsoids drawn at 50% probability. All hydrogens and lattice waters are omitted for clarity. (Symmetry codes: A: x, $-1/2-y$, $1/2+z$; B: x, $\frac{1}{2}-y$, $-1/2+z$).

are in agreement with those found in a Cu(II)–trza$^-$ complex [16]. The Cu(II) ion lies 0.099 Å above the mean plane of four equatorial donor atoms and is oriented toward the apex of the pyramid occupied by the water molecule with Cu–O5 bond length of 2.514(5) Å. Unlike the free ligand, trzp$^-$ adopts two different conformations (*gauche* and *trans*) in **1**. In the distorted *gauche* conformer, the N1–C3–C4–C5 torsion angle is 88.5(8)°, and in the *trans* conformer, the torsion angle is −175.9(6)°. Both two-connected conformers bridge Cu(II) atoms alternately in two different directions, through the triazole group at the one end and carboxylate group at the other, to give 1-D coordination chains. These 1-D chains are interwoven into a 2-D network with (4,4) topology in the *bc* plane (figure 4). A quadrilateral grid consisting of four Cu(II) atoms and four trzp$^-$ bridges can be regarded as the repeating structural unit in the 2-D layer, in which the *gauche* conformers are close to each other, as well as the *trans* conformers. The Cu···Cu distance across the *gauche* conformer is 9.189 Å and that *via* the *trans* conformer is 10.452 Å. The diagonal distances of the grid are 13.175 and 14.500 Å. Furthermore, the 2-D polymeric sheets are stacked in an offset ABAB manner running along the *a* axis *via* π–π interactions between the parallel triazole rings (centroid–centroid distance = 3.571 Å). O–H···O and O–H···N hydrogen bonds between lattice waters and 2-D sheets help stabilize the 3-D supramolecular framework (figure 5).

3.1.3. Crystal structure of $\{[Co(trzp)_2(H_2O)_2]\cdot 2H_2O\}_n$ (2). Complex **2** crystallizes in the monoclinic system with space group $P2_1/c$. The Co(II) ion is on an inversion center, and it is coordinated by two triazole N atoms (N3B and N3C) and two carboxylate O atoms (O1 and O1A) from four separate trzp$^-$ ligands, and two O atoms of water molecules (O3 and O3A), yielding a nearly regular octahedral coordination sphere (figure 6). The Co–N and Co–O bond distances in the CoN_2O_4 polyhedron are nearly equivalent and comparable to the values found for related Co(II) complexes [16, 17]. Unlike **1**, only one crystallographically independent trzp$^-$ ligand with *trans* conformation exists in the asymmetric unit, and the torsion angle about the central C3–C4 bond is 166.9(3)°. Each

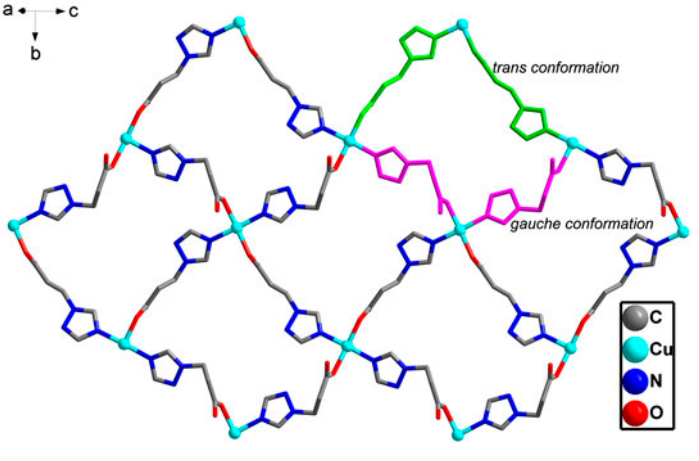

Figure 4. The 2-D (4,4) coordination layer of **1** extending along the crystallographic *bc* plane. A rhombohedral grid is highlighted with the ligands in green adopting a *trans* conformation and the ligands in purple adopting a *gauche* conformation. Coordinated waters are omitted for clarity (see http://dx.doi.org/10.1080/00958972.2013.807919 for color version).

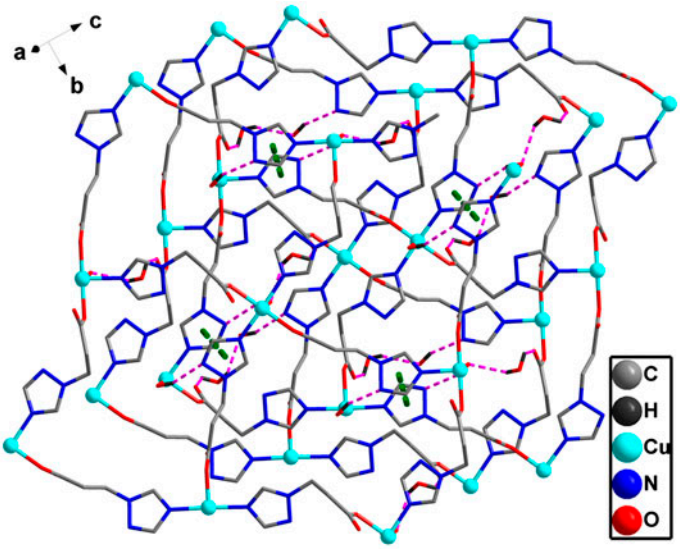

Figure 5. The 3-D supramolecular network of **1** generated *via* π–π interactions and hydrogen bonds (dashed lines).

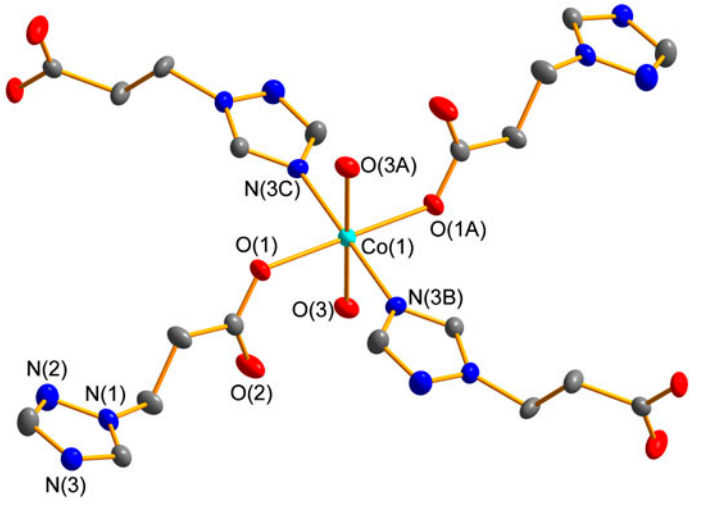

Figure 6. The coordination environment of Co(II) in **2** with thermal ellipsoids drawn at 50% probability. All hydrogens and lattice waters are omitted for clarity. (Symmetry codes: A: $-1-x$, $1-y$, $-z$; B: $-1+x$, $\frac{1}{2}-y$, $-1/2+z$; C: $-x$, $1/2+y$, $\frac{1}{2}-z$).

$trzp^-$ ligand behaves as a two-connected linker joining two neighboring Co(II) ions, resulting in a 2-D planar sheet of (4,4) topology parallel to the (1 0 −2) plane (figure 7). Within the 2-D sheet, the nearest Co···Co separation *via* the bridging $trzp^-$ is 10.366 Å. Water molecules are contained within this 2-D lattice framework through O–H···O hydrogen bonding interactions with the neighboring layers. Face-to-face π–π interaction (centroid–centroid distance = 3.778 Å) between triazole moieties as well as O–H···N hydrogen bonds assembles 2-D sheets into a 3-D supramolecular matrix (figure 8).

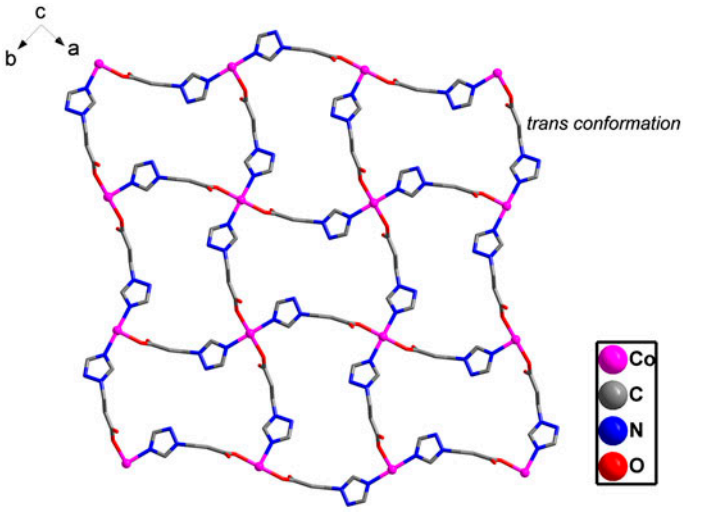

Figure 7. The 2-D (4,4) coordination network of **2** viewed down the *c* axis. Coordinated waters are omitted for clarity.

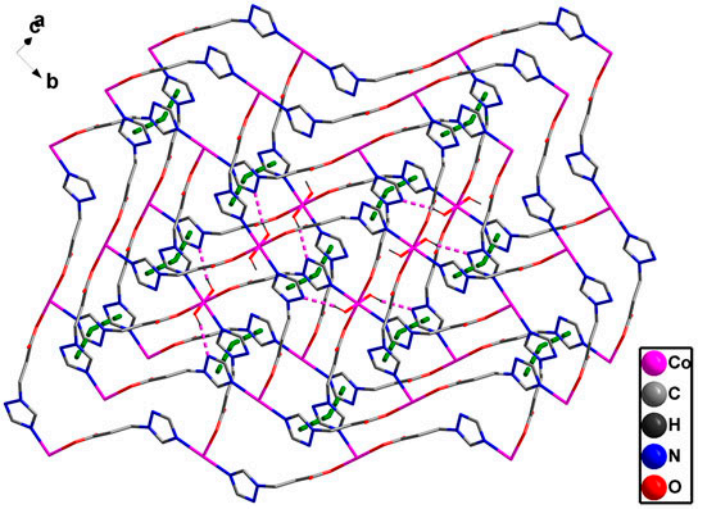

Figure 8. The solid-state 3-D supramolecular structure of **2** supported by π–π interactions and hydrogen bonds (dashed lines).

3.1.4. Crystal structure of $\{[Cd(trzp)_2(H_2O)]\cdot 2H_2O\}_n$ (3). Complex **3** also has a 2-D layered coordination network constructed by $trzp^-$ ligands in a *trans* conformation (N1–C3–C4–C5 torsion angle = −170.0(2)°) bridging Cd(II) ions, and the structure is roughly analogous to that of **2**. There are two major structural differences between **2** and **3**. First, the central Cd(II) ion has a seven-coordinate pentagonal bipyramidal geometry, consisting of five O donors (O1, O2, O1A, O2A, and O3) from two equivalent $trzp^-$ carboxylate groups and one coordinated water in the equatorial positions, and two triazole N atoms (N3C and N3B) from another two $trzp^-$ ligands in the axial positions (figure 9).

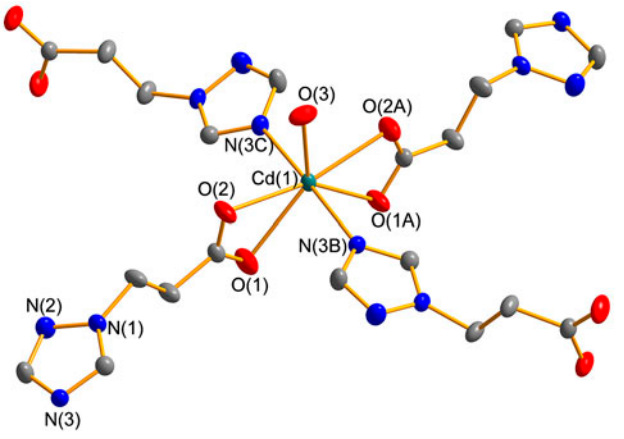

Figure 9. The coordination environment of Cd(II) in **3** with thermal ellipsoids drawn at 50% probability. All hydrogens and lattice waters are omitted for clarity. (Symmetry codes: A: $1-x$, y, $-1/2-z$; B: $\frac{1}{2}-x$, $\frac{1}{2}-y$, $-1/2+z$; C: $1/2+x$, $\frac{1}{2}-y$, $-z$).

The Cd–N bond length is 2.320(2) Å, and the Cd–O bond lengths of the asymmetrically chelating carboxylate are 2.366(3) and 2.501(2) Å. These bond parameters are comparable to the reported values for Cd(II)-azole and Cd(II)-carboxylate complexes [18, 27]. Second, the trzp$^-$ bridge is tridentate with its carboxylate functional group chelating to one Cd(II) ion, whereas the triazole moiety binds to a second Cd(II) ion (figure 10). The separation between two nearest neighbor Cd(II) ions is 10.414 Å. π–π stacking (centroid–centroid distance = 3.690 Å) and hydrogen bond interactions also play important roles in consolidating the 3-D supramolecular architecture along the crystallographic *b* direction.

3.1.5. Crystal structure of $[Ag_3(trzp)_2(NO_3)]_n$ (4). Complex **4** exhibits a complicated 3-D polymeric structure, clearly different from the previously reported analogous compound $[Ag_{1.5}(trza)(NO_3)_{0.5}]_n$ [18], which may be ascribed to the larger structural flexibility

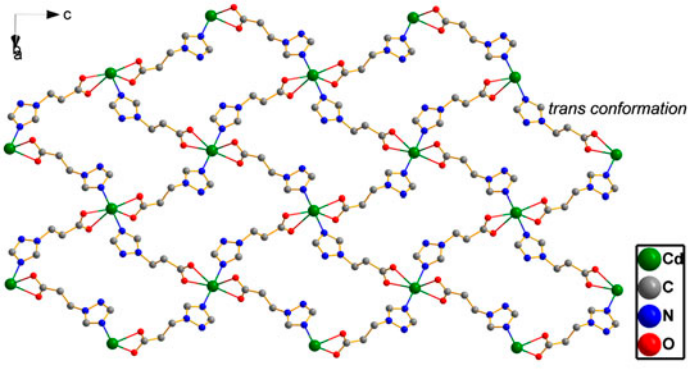

Figure 10. The 2-D (4,4) coordination network of **3** extending along the crystallographic *ac* plane. Coordinated waters are omitted for clarity.

of $trzp^-$ as contrasted with $trza^-$. There are two chemically independent Ag(I) atoms (Ag1 and Ag2) in the asymmetric unit of **4**. The formally anionic Ag1 is tetrahedrally bonded to three $trzp^-$ ligands via two carboxylate O atoms (O1C and O2B), one triazole N atom (N2), and a nitrate anion. The formally cationic Ag2 is in a linear geometry, capped by two triazole N atoms (N3 and N3D) from two different $trzp^-$ (figure 11). The Ag1–O(carboxylate) bond distances (2.286(4) and 2.290(4) Å) are in the expected range [18] and much shorter than Ag1–O3A(nitrate) bond distance (2.60(3) Å). The Ag1–N2 bond length of 2.424(5) Å is typical for tetrahedral Ag(I) complexes [19], but considerably longer than the distance between N3 and Ag2 (2.189(4) Å) [20]. The difference between the two bond lengths reflects the greater steric constraints imposed on the central atom by tetrahedral geometry than those imposed by a linear coordination environment. The $trzp^-$ ligand in **4** possesses a *gauche* conformation (N1–C3–C4–C5 torsion angle = −68.7(6)°) and it connects to three Ag1 and one Ag2, making use of its terminal bidentate carboxylate group and bridging triazole ring. A pair of $trzp^-$ coordinate with μ_2-bridging carboxylate groups to couple two neighboring Ag1, yielding a dinuclear $[Ag_2(COO)_2]$ subunit with a Ag···Ag separation of 2.974 Å. The distance is shorter than the sum of the van der Waals radii of two Ag atoms and in agreement with the Ag···Ag distance (2.970 Å) found in the related

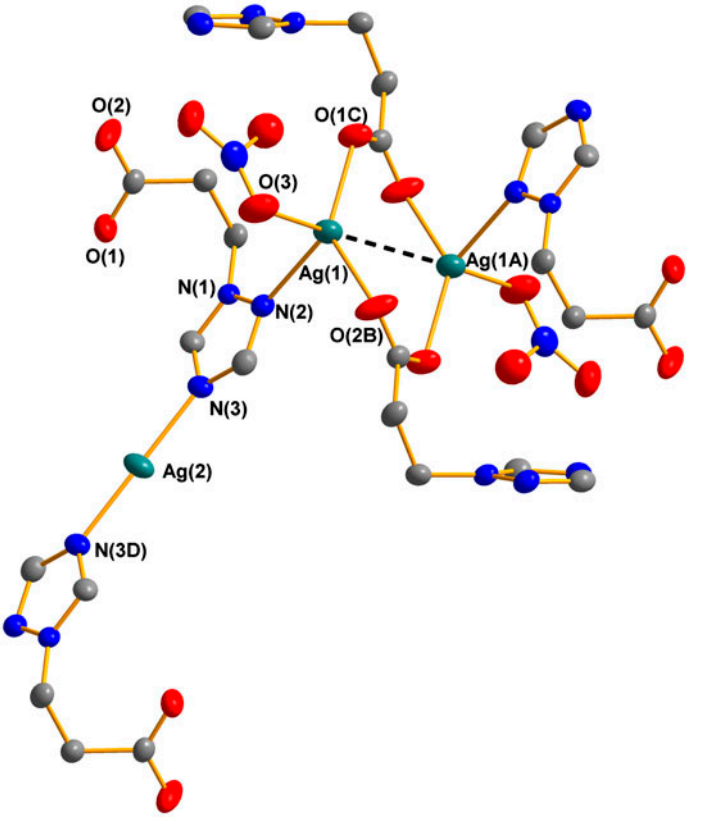

Figure 11. The coordination environments of Ag(I) in **4** with thermal ellipsoids drawn at 50% probability. All hydrogens are omitted for clarity. (Symmetry codes: A: ½ − *x*, 5/2 − *y*, 1 − *z*; B: *x*, 2 − *y*, 1/2 + *z*; C: ½ − *x*, 1/2 + *y*, ½ − *z*; D: 1 − *x*, 1 − *y*, 1 − *z*).

compound $[Ag_{1.5}(trza)(NO_3)_{0.5}]_n$ [18], indicative of the formation of a metal–metal interaction. Each $[Ag_2(COO)_2]$ subunit is cross-linked with four identical subunits *via* N2 of the triazole rings, resulting in a 2-D metal–organic network parallel to the crystallographic *bc* plane, in which the triazole groups protrude alternatively up and down from the layer (figure 12). Furthermore, the 2-D layers extend into a complicated 3-D cationic framework (figure 13) through the binding of Ag2 with triazole N3 from two adjacent layers. The 3-D framework presents irregular tubular channels along the crystallographic *b* axis. Complex **4** can be considered to be formally zwitterionic or that the weakly coordinating nitrate anions are incorporated into the channels to balance the positive charge of the framework.

Other coordination polymers with different topologies have been prepared by an analogous triazole-carboxylic acid ligand Htrza with a shorter methylene spacer [16, 18]. It is meaningful to compare the structural features of these previously reported complexes with the complexes based on the more flexible Htrzp. The crystal structures of **1** and **2** reveal 2-D (4,4) topology networks which are remarkably similar to those reported for the $trza^-$ complexes of Cu(II) and Co(II) [16]. However, the 2-D (4,4) topology structure of **3** is different from that of the Cd(II)-$trza^-$ complex, in which Cd(II) atoms are joined by the three-connected $trza^-$ into a 2-D (6,3) network [16]. Also, **4** exhibits a 3-D polymeric architecture quite different from the 2-D puckered layer structure of the Ag(I)–$trza^-$ complex [18]. These results demonstrate that in some cases flexible spacers of different lengths can cause structural changes in coordination polymers with the triazole-carboxylic acid ligands.

3.2. *IR spectra of ligand and complexes*

The IR spectra (figure S1) of **1**–**4** are almost identical, but there are some obvious differences with that of Htrzp. The IR spectrum of Htrzp exhibits a sharp band around 3131 cm^{-1}, corresponding to the azole ring C–H stretching vibration [28]. The weak broad absorptions observed in the spectral region 2900–3050 cm^{-1} are attributed to the O–H stretching of carboxylic group and to the C–H stretching of the ethylene moiety. An intense band at 1705 cm^{-1} is indicative of the C = O stretch vibration of the carboxylic acid. The azole ring stretching bands can be found at 1523 and 1429 cm^{-1} [28]. A strong

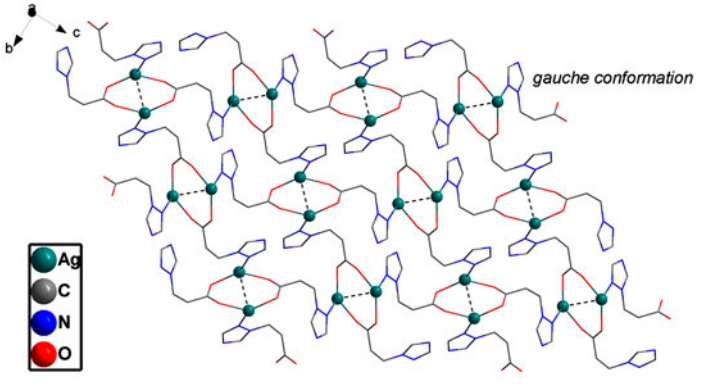

Figure 12. The 2-D network of **4** viewed from the crystallographic *a* axis with Ag···Ag interactions indicated by dashed lines.

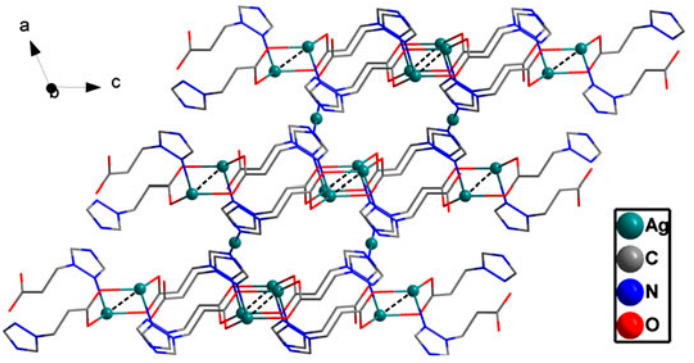

Figure 13. A view of the overall 3-D polymeric structure of **4** down the *b* axis with Ag···Ag interactions indicated by dashed lines.

band centered at 1232 cm^{-1} arises from the C–O stretching mode of the carboxylic acid [29]. Upon complexation, the presence of the deprotonated carboxylate group of $trzp^-$ is illustrated by the disappearance of the C=O stretching band in the IR spectra of **1**–**4**. In addition, the spectra of **1**–**4** show characteristic bands for the carboxylate group at 1583, 1574, 1590, and 1582 cm^{-1}, respectively, for the asymmetric stretching vibration. The symmetric stretching bands of the carboxylate group can be seen in the spectral region of 1390–1440 cm^{-1} for **1**–**3**. For **4**, this band overlaps with the strong absorption of the nitrate anion at 1384 cm^{-1}.

3.3. *PXRD determination*

Polycrystalline samples of **1**–**4** were subjected to X-ray powder diffraction (PXRD) analysis to examine the crystallinity and phase purity. The experimental and simulated PXRD patterns of **1**–**4** are depicted in figure S2. Only slight differences can be found between the experimental patterns and the simulated ones, which confirm the excellent phase purity of the as-synthesized samples.

3.4. *Thermogravimetry analysis*

The TGA were recorded on crystalline samples in an N_2 atmosphere to evaluate the thermal stability of **1**–**4** (figure S3). The thermal decomposition pattern of **1** displayed three well-defined degradation stages. The first stage, from 40 to 170 °C with an observed weight loss of 10.25% (Calcd: 11.58%), corresponds to removal of 2.18 water molecules per formula unit. Upon heating from 230 to 380 °C, **1** showed two abrupt weight decreases associated with the partial combustion of the heterocyclic ligands. The product formed at 380 °C accounts for 30.00% of the total sample weight, consistent with the formation of $Cu(CN)_2$ (Calcd: 30.17%) [30].

The TG curve of **2** exhibited an initial weight loss of 17.61% between 70 and 160 °C, denoting the release of two lattice water and two coordinated water molecules (Calcd: 17.52%). There was a stable plateau between 160 and 250 °C, followed by a second weight loss of 34.79% between 250 and 390 °C, which is consistent with the elimination of the $CH_2CH_2COO^-$ moieties (Calcd: 35.05%). The subsequent weight loss step between

390 °C and 480 °C is ascribed to the partial combustion of the triazole ring to give the product $Co(CN)_2$ (obsd: 28.11%; Calcd: 26.98%). Above 480 °C, a gradual mass loss was observed, tentatively assigned to the degradation of $Co(CN)_2$.

For **3**, the TG profile showed a weight loss between 55 and 170 °C, corresponding to the loss of the three water molecules (obsd: 12.00%; Calcd: 12.10%). The framework of **3** collapses gradually above 260 °C, but the combustion process could not be separated into distinct steps. At 800 °C, the residual weight percentage is 35.77%, in agreement with a composition of $Cd(CN)_2$ (Calcd: 36.81%).

The metal–organic framework of **4** is thermally stable until the first rapid decomposition occurs at 210 °C, with a weight loss consistent with the elimination of $CH_2CH_2COO^-$ (obsd: 21.69%; Calcd: 21.64%). The following weight loss between 260 and 350 °C with a value of 14.01% corresponds to loss of part of the remaining $trzp^-$ (Calcd: 12.62%), leaving a mixture of $AgNO_3$ and AgCN.

4. Conclusions

Four transition metal-organic coordination polymers with the conformationally flexible ligand 1*H*-1,2,4-triazole-1-propionic acid have been obtained. For Cu(II), Co(II), and Cd (II), each bifunctional $trzp^-$ bridges two metal centers *via* the terminal triazole ring and carboxylate, resulting in similar 2-D (4,4) networks. In contrast, the multidentate linker is bonded to four Ag(I) ions to produce a 3-D framework. The flexible ligand adopts a *trans* conformation in **2** and **3**, a *gauche* conformation in **4,** and both conformations in **1**. Hence, the structural and topological changes of these complexes stem mainly from the different connectivity of the multidentate bridging ligand. In the present study, the conformational change of the flexible organic linker has no substantial influence on the topological networks made from Cu(II), Co(II), and Cd(II) with different coordination requirements. Structural variation can, however, be achieved by choosing triazole-carboxylic acids with different flexible spacers.

Supplementary material

IR, PXRD, and TGA data for **1**–**4**. CCDC 906425 and 854953–854956 contain the Supplementary crystallographic data for the compounds reported in this paper. Copies of this information can be obtained free of charge from the Cambridge Crystallographic Data Center *via* http://www.ccdc.cam.ac.uk/conts/retrieving.html, or from the Cambridge Crystallographic Data Center, 12 Union Road, Cambridge CB2 1EZ, UK; Fax: +44 1223 336 033 or E-mail: deposit@ccdc.cam.ac.uk.

Acknowledgements

This work was financially supported by the Guangxi Natural Science Foundation of China (grant no. 2010GXNSFF013001, 0832023) and Scientific Research Foundation of Guangxi Normal University.

References

[1] S.T. Meek, J.A. Greathouse, M.D. Allendorf. *Adv. Mater.*, **23**, 249 (2011).
[2] N. Stock, S. Biswas. *Chem. Rev.*, **112**, 933 (2012).

[3] T.F. Liu, J. Lu, C. Tian, M. Cao, Z. Lin, R. Cao. *Inorg. Chem.*, **50**, 2264 (2011).
[4] B. Ding, Y.Y. Liu, Y.Q. Huang, W. Shi, P. Cheng, D.Z. Liao, S.P. Yan. *Cryst. Growth Des.*, **9**, 593 (2009).
[5] S.C. Chen, Z.H. Zhang, Y.S. Zhou, W.Y. Zhou, Y.Z. Li, M.Y. He, Q. Chen, M. Du. *Cryst. Growth Des.*, **11**, 4190 (2011).
[6] B.X. Dong, X.J. Gu, Q. Xu. *Dalton Trans.*, **39**, 5683 (2010).
[7] G.X. Liu, H. Xu, H. Zhou, S. Nishihara, X.M. Ren. *CrystEngComm.*, **14**, 1856 (2012).
[8] D. Zhao, D.J. Timmons, D. Yuan, H.C. Zhou. *Acc. Chem. Res.*, **44**, 123 (2011).
[9] B. Ding, L. Yi, P. Cheng, D.Z. Liao, S.P. Yan. *Inorg. Chem.*, **45**, 5799 (2006).
[10] Q.G. Zhai, X.Y. Wu, S.M. Chen, Z.G. Zhao, C.Z. Lu. *Inorg. Chem.*, **46**, 5046 (2007).
[11] W. Ouellette, A.V. Prosvirin, J. Valeich, K.R. Dunbar, J. Zubieta. *Inorg. Chem.*, **46**, 9067 (2007).
[12] D.P. Li, X.H. Zhou, X.Q. Liang, C.H. Li, C. Chen, J. Liu, X.Z. You. *Cryst. Growth Des.*, **10**, 2136 (2010).
[13] L. Tian, L. Yan. *J. Coord. Chem.*, **65**, 1600 (2012).
[14] Q. Lin, T. Wu, S.T. Zheng, X. Bu, P. Feng. *Chem. Commun.*, **47**, 11852 (2011).
[15] L.R. Jia, M. Hu, S.M. Fang, C.S. Liu. *J. Coord. Chem.*, **64**, 1849 (2011).
[16] X.Y. Zhou, Y.Q. Huang, W.Y. Sun. *Inorg. Chim. Acta*, **362**, 1399 (2009).
[17] N.V. Fischer, A. Inayat, W. Schwieger, N. Burzlaff. *J. Coord. Chem.*, **63**, 2831 (2010).
[18] D.G. Ding, L.X. Xie, Y.T. Fan, H.W. Hou, Y. Xu. *J. Solid State Chem.*, **182**, 1443 (2009).
[19] L.X. Xie, A.M. Ning, X. Li. *J. Coord. Chem.*, **62**, 1604 (2009).
[20] T.L. Hu, W.P. Du, B.W. Hu, J.R. Li, X.H. Bu, R. Cao. *CrystEngComm.*, **10**, 1037 (2008).
[21] B. Ding, E.C. Yang, J.H. Guo, X.J. Zhao, X.G. Wang. *Inorg. Chem. Commun.*, **11**, 1481 (2008).
[22] B.W. Hu, J.P. Zhao, Q. Yang, F.C. Liu, X.H. Bu. *J. Mater. Chem.*, **19**, 6827 (2009).
[23] X.L. Tong, J.H. Xin, W.H. Guo, X.P. Zhu. *J. Coord. Chem.*, **64**, 2984 (2011).
[24] V. Safarifard, A. Morsali. *CrystEngComm.*, **13**, 4817 (2011).
[25] R.H. Wiley, N.R. Smith, D.M. Johnson, J. Moffat. *J. Am. Chem. Soc.*, **77**, 2572 (1955).
[26] G.M. Sheldrick. *Software Package SHELXTL V6.1 for Structure Solution and Refinement*, Bruker AXS, Inc., Madison, Wisconsin, USA (2000).
[27] J.H. Lun, F.L. Jiang, R.H. Wang, L. Han, Z.Z. Lin, R. Cao, M.C. Hong. *J. Mol. Struct.*, **707**, 211 (2004).
[28] D. Bougeard, N. Le Calve, B.S. Roch, A. Novak. *J. Chem. Phys.*, **64**, 5152 (1976).
[29] Y. Mikawa, J.W. Brasch, R.J. Jakobsen. *J. Mol. Struct.*, **3**, 103 (1969).
[30] W. Ouellette, B.S. Hudson, J. Zubieta. *Inorg. Chem.*, **46**, 4887 (2007).